

Optimized Ratiometric Calcium Sensors for Functional *In Vivo* Imaging of Neurons and T-Lymphocytes

Thomas Thestrup, Julia Litzlbauer, Ingo Bartholomäus, Marsilius Mues, Luigi Russo, Hod Dana, Yuri Kovalchuk, Yajie Liang, Georgios Kalamakis, Yvonne Laukat, Stefan Becker, Gregor Witte, Anselm Geiger, Taylor Allen, Lawrence C Rome, Tsai-Wen Chen, Douglas S. Kim, Olga Garaschuk, Christian Griesinger, Oliver Griesbeck

Supplementary materials

Supplementary Figure 1	Sequence alignment of various TnCs used for indicator construction
Supplementary Figure 2	Comparison of TN-L15 and Ts-L13 off-kinetics
Supplementary Figure 3	Incorporating the minimal domain into FRET sensors - Initial engineering of FRET change with small proline linker libraries
Supplementary Figure 4	NMR characterization of calcium loaded tsTnC minimal domain and ^1H - ^{15}N HSQC spectra used to monitor the Ca^{2+} and Mg^{2+} binding affinity.
Supplementary Figure 5	The structure of the tsTnC minimal domain compared to the C-terminal domain of Chicken TnC
Supplementary Figure 6	Measured SAXS curves of the sensors in absence and presence of calcium
Supplementary Figure 7	SAXS multi-domain modeling
Supplementary Figure 8	Diversified indicator libraries generated for screening
Supplementary Figure 9	Bacterial colony screening
Supplementary Figure 10	Comparison of selected FRET calcium sensors in dissociated neurons
Supplementary Figure 11	<i>In vivo</i> functional imaging of mouse visual cortex using Twitch-3
Supplementary Figure 12	Differences in baseline fluorescence between Twitch-3 and YC3.60 <i>in vivo</i>

Supplementary Figure 13	Emission spectra of purified “Twitch” variants <i>in vitro</i>
Supplementary Table S1	NMR structural statistics
Supplementary Table S2	SAXS data evaluation
Supplementary Table S3	Construct Overview

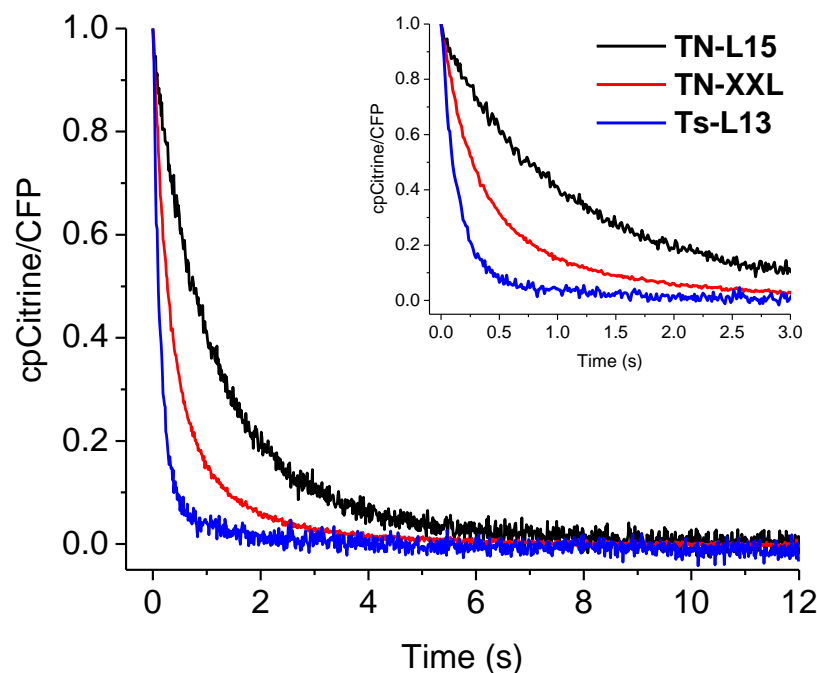
Supplementary Figure 1. Sequence alignment of various TnCs tested for indicator construction.



Sequence alignment of different TnC variants and calmodulin used as parental genes for construction of new calcium indicators. All indicated TnCs could be sandwiched between donor and acceptor FPs and yielded FRET sensors with varying FRET changes and Kds (data not shown). Sensors based on C-terminal lobe domains generally had higher calcium affinities than sensors based on full-length sequences or on N-terminal lobe domains. The red color indicates functional EF-hand domains whereas grey indicates non-functional domains. *Structure** illustrates the approximate position of the helices (grey helix) and β -sheets (blue arrow) in troponin c and calmodulin.

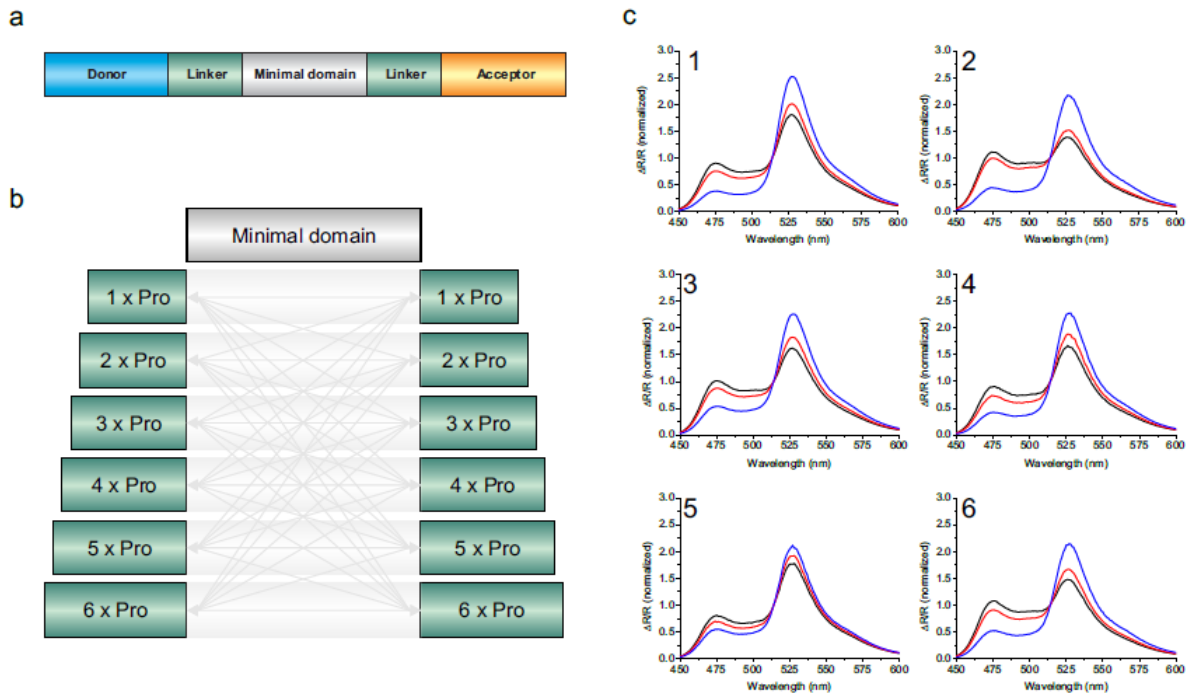
* The CaBP Data Library – Troponin C (accessed 14.07.08) http://structbio.vanderbilt.edu/cabp_database/general/prot_pages/tropc.html

Supplementary Figure 2. Comparison of TN-L15 and Ts-L13 off-kinetics.



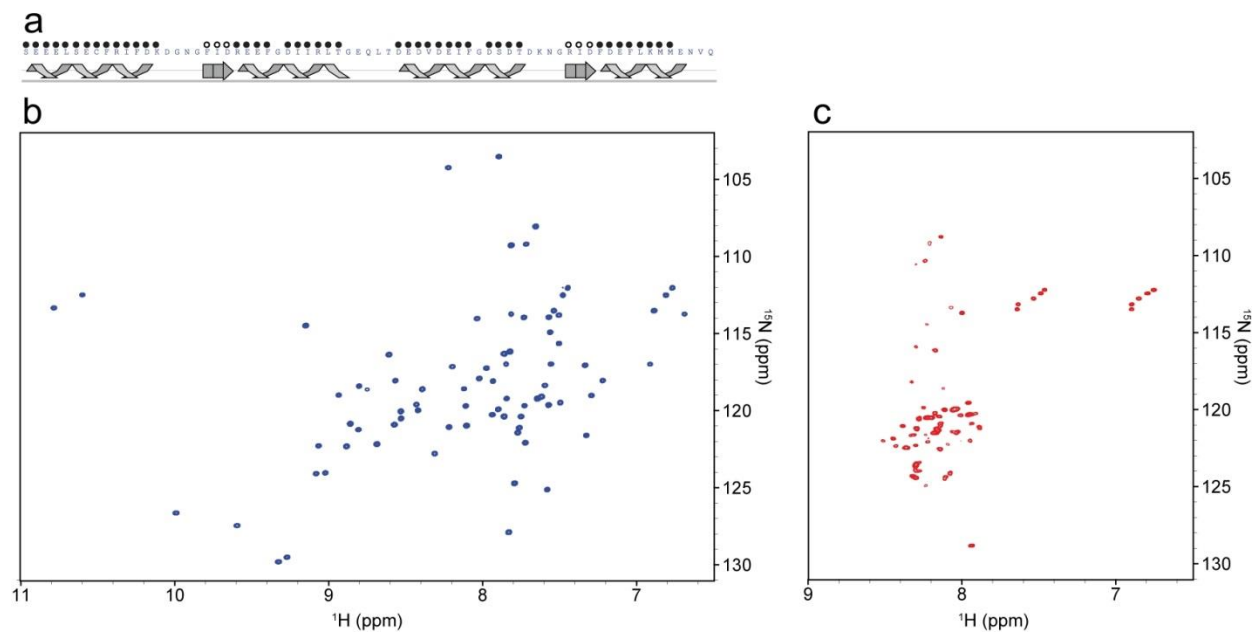
TN-L15 and Ts-L13 are simple FRET sensors based on wildtype chicken TnC truncated at leucin 15 (TN-L15) (Heim & Griesbeck, 2004) or toadfish white muscle/swim bladder TnC truncated at leucin 13 (Ts-L13). Both sensors based on the wild type proteins comprising both the N- and C-terminal domains had comparable calcium affinities of 1.2 and 1.3 μM , respectively. Shown are *in vitro* stopped flow kinetics show calcium off-rates from the indicators TN-L15 ($\tau = 1.230$ s), TN-XXL ($\tau = 0.527$ s) and ts-L13 ($\tau = 0.178$ s), taken at room temperature. The inlay shows a zoom in from 0-3 seconds. The experiments were conducted by mixing calcium saturated indicators with the strong calcium chelator BAPTA, and following the time course of signal relaxation. The two solutions were prepared as following: Calcium saturated indicator (5 ml): 10 mM MOPS, 4 mM CaCl_2 , 1 mM MgCl_2 , 50 mM KCl, $\sim 0.2 - 1$ μM indicator pH 7.5 and mixed with BAPTA solution (5 ml): 10 mM MOPS, 50 mM KCl, 20 mM BAPTA pH 7.5.

Supplementary Figure 3. Sandwiching the minimal domain into FRET sensors. Initial engineering of FRET change with small proline linker libraries.



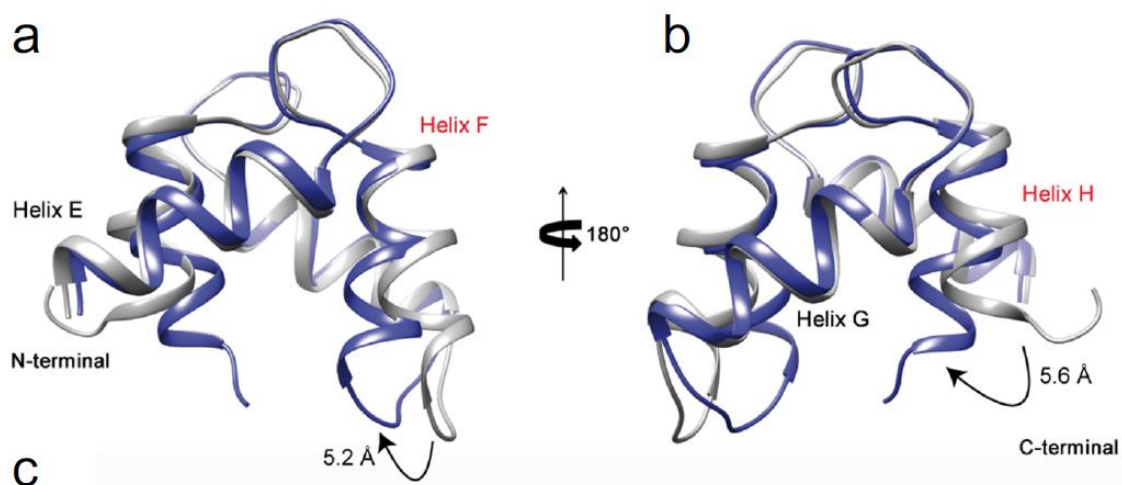
(a) A schematic representation of the sensor design in which the minimal calcium binding domain (grey) is sandwiched via amino acid linkers (green) between a donor (blue) and acceptor (yellow) fluorescent protein (b) Effects of linker insertions consisting of 0-6 prolines on basal and calcium induced FRET. A total of 49 sensors were assayed with combinations of 0-6 prolines at the N-terminal and C-terminal ends of the minimal domain. The light grey arrows indicate the different combinations. (c) Figure C1-C6 illustrates the differences in starting ratio and FRET change for a selection of sensors with proline linkers (C1: 1,1 Pro, C2: 2,2 Pro, C3: 3,3 Pro, C4: 4,2 Pro, C5: 6,0 Pro and C6: 2,5 Pro). Black lines represent the calcium free state, red; Mg^{2+} sensitivity (1 mM Mg^{2+}) and blue line the maximum calcium response (10 mM Ca^{2+}). C1 became the basis for the design of Twitch-1.

Supplementary Figure 4. NMR characterization of calcium loaded tsTnC minimal domain and ^1H - ^{15}N HSQC spectra used to monitor the Ca^{2+} and Mg^{2+} binding affinity.



(a) Secondary structure elements in dependence of the sequence in tsTnC minimal domain as derived by the Chemical Shift Index (CSI) based on $\text{C}\beta$ resonance assignments. $^3\text{J}_{\text{H}_\text{N}\text{H}_\alpha}$ coupling constants are also reported and indicated by filled and open circles for values of $^3\text{J}_{\text{H}_\text{N}\text{H}_\alpha} < 4.5$ Hz or > 8 Hz, respectively. ^1H - ^{15}N heteronuclear single quantum correlation (HSQC) spectra of tsTnC minimal domain in Calcium saturated **(b)** and calcium free forms in presence of magnesium **(c)**.

Supplementary Figure 5. The structure of the tsTnC minimal domain compared to the C-terminal domain of Chicken TnC.



Protein	Interhelical angles (°) ¹			
	Helix E / Helix F	Helix F / Helix G	Helix G / Helix H	Helix E / Helix H
tsTnC minimal domain ²	120 ± 4	111 ± 7	132 ± 7	102 ± 5
C domain of Chicken TnC (X-ray) ³	106	125	113	115
Protein	Interhelical distances (Å) ¹			
	Helix E / Helix F	Helix F / Helix G	Helix G / Helix H	Helix E / Helix H
tsTnC minimal domain ²	13.7 ± 0.4	10.9 ± 0.9	13.0 ± 0.8	10.3 ± 0.5
C domain of Chicken TnC (X-ray) ³	15.6	11.3	14.1	10.8

¹Calculated using the software Interhix written by Kyoko Yap and Mitsuhiro Ikura (University of Toronto).

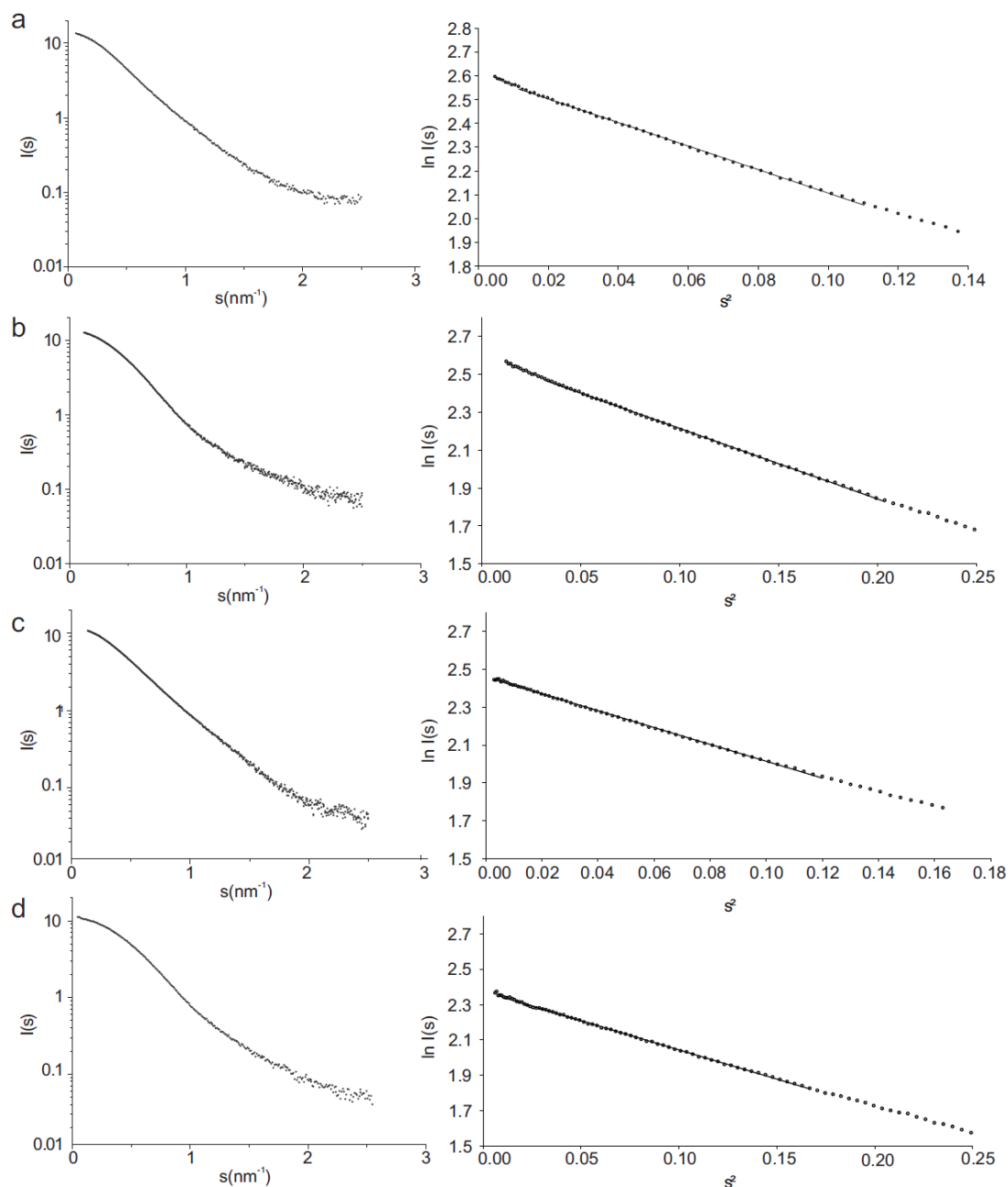
Helices E/F and G/H correspond to the helices forming calcium binding site EF3 and EF4, respectively.

²Listed are the mean ± standard error values calculated for twenty structures.

³PDB accession code: 1TOP. Helices are defined in the PDB file

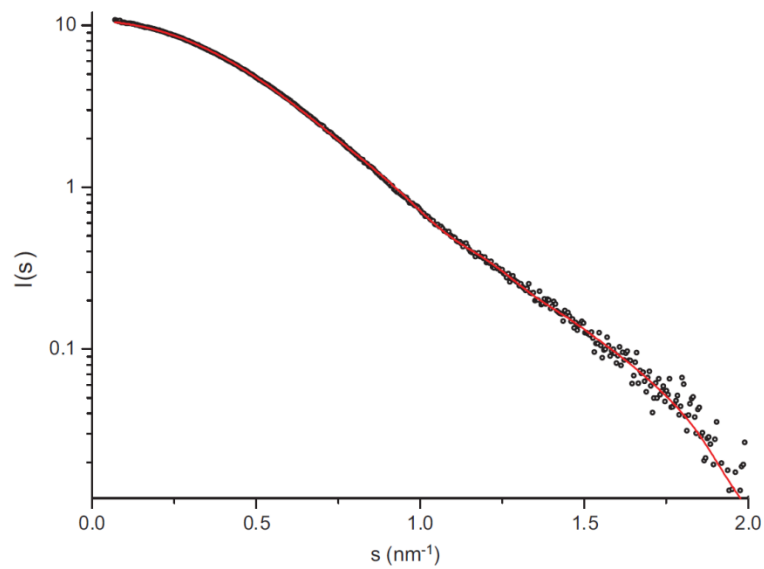
(a)-(b) Comparison of the average NMR structure of tsTnC minimal domain (*blue*) and the C-terminal domain of Chicken TnC (Protein Data Bank ID code: 1TOP) (*gray*) after superposition on the backbone atoms in two different orientations rotated 180° around z axis. (c) Helix-Helix angles and distances for the tsTnC minimal domain and C-terminal lobe domain of Chicken TnC. The two structures adopt a similar fold ($rmsd_{bb} = 2.9 \text{ \AA}$), in which the secondary structure is conserved while the tertiary structure displays significant differences. We quantified the structural dissimilarity by measuring the interhelical angles. As reported in table (C) the minimal domain adopts a conformation in which the slight opening of the calcium binding loops drives the domain closing in a more compact four-helix bundle. Furthermore, the magnitude of the movement of helices F and H is characterized by a change in interhelical distance, resulting in displacements of 5.2 Å for the C-terminal end of helix F (A) and 5.6 Å for the C-terminal end of helix H.

Supplementary Figure 6. Measured Small-Angle X-ray Scattering curves of the sensors in absence and presence of calcium.



All curves show the buffer corrected scattering curves (left) and the corresponding Guinier-plot ($\ln I(s)$ vs. s^2) with linear region used for determination of R_g with $s \cdot R_g < 1.3$ (right). **(a)** Twitch-0 without calcium, $R_g=3.84$ nm **(b)** Twitch-0 in presence of calcium, $R_g=3.35$ nm **(c)** Twitch-1 without calcium, $R_g=3.65$ nm **(d)** Twitch-1 in presence of calcium, $R_g=3.14$ nm. The comparison of a and b or c and d, respectively, show a change in shape to a more globular particle upon calcium binding.

Supplementary Figure 7. SAXS multi-domain modeling.



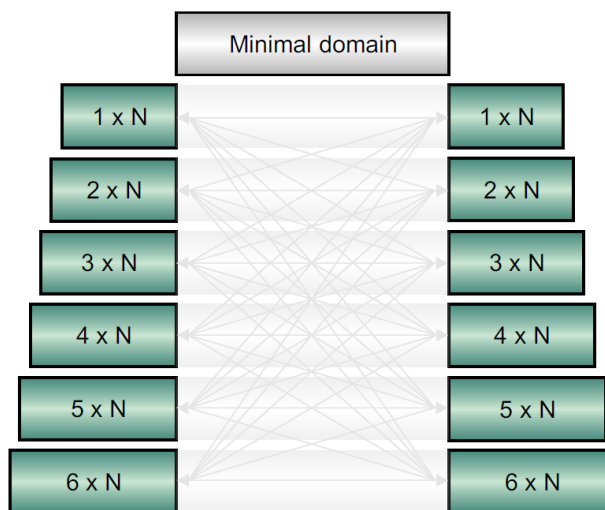
Fit of the modeled structure (see figure 2d in main text) of the calcium bound states of Twitch-1. Multi-domain modeling was performed using CORAL (Petoukhov, M.V. & Svergun, D.I., 2005) with ECFP (pdb code 2WSN), Citrine (pdb code 3DPX) and the structure of the calcium loaded minimal domain (this paper) and the respective scattering curves of calcium bound Twitch-1. To allow structural changes at the connecting termini of the fluorescent proteins induced by calcium binding to the minimal domain a “flexible linker stretch” of up to 5 residues was allowed for CORAL modeling to avoid clashes.

Supplementary Figure 8. Diversified indicator libraries generated for screening.

a

Helix	EF-hand
L5	K14
F9	G16
F12	N17
E23	G18
I28	F19
V41	I20
I44	D21
F45	R22
S48	D57
F58	
M64	
M65	
V68	

c

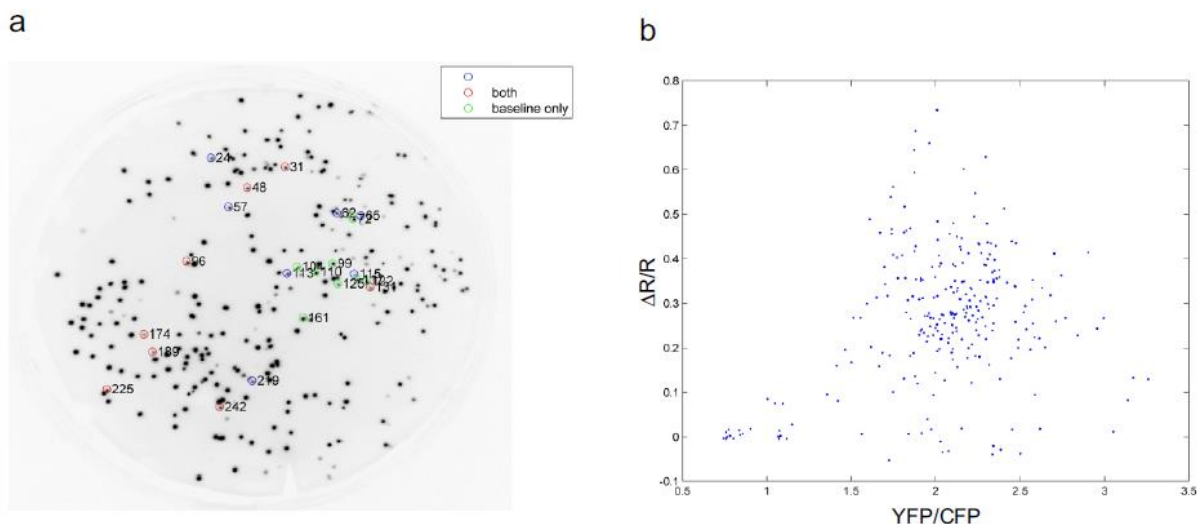


b

SEEELSECFRIFDKDGNGFIDREEFGDIIRLTGEQLTDEDVDEIFGSDTDKNGRIDDDEFLLKMENVQ

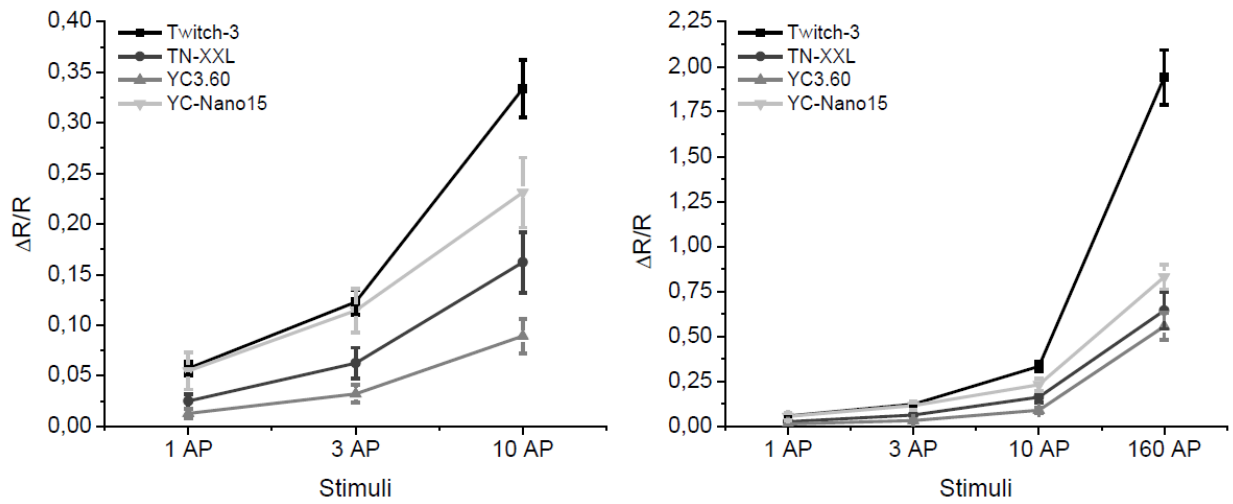
Summary of Twitch libraries based on hotspot mutations within the minimal domain and diversified linkers, as well as combinations hereof. **(a)** Several structural hotspots were identified through close examination of the C-lobe structure (see figure 2 of the main text). Both helix- (grey) and EF-hand (light green) residues were targeted to optimize calcium induced FRET change and calcium affinities. Three key mutation sites, K14, V41 and M65, are shown in large bold fonts, as they had significant effects on overall FRET change. **(b)** Amino acid sequence of the minimal calcium binding domain. K14, V41 and M65 are marked with bold and underscore, helices (grey) and EF-hand mutations (light green). For their localization within the structure see also figure 2 in the main text **(c)** To generate large scale diversified linker libraries, cassettes of 1-6 random linking amino acids were added to the N-terminal and C-terminal end of the minimal calcium binding domain as shown in B and sandwiched between donor and acceptor fluorescent proteins. N = random amino acid residue.

Supplementary Figure 9. Bacterial plate screening.



Diversified Twitch sensor libraries were transformed into *E. coli* XL1 Blue, plated on Agar plates and screened for basal starting ratio and calcium induced FRET change via CCD camera wide field imaging. **(a)** False color representation of an Agar plate with bacterial colonies each expressing a diversified Twitch sensor variant. Up to 1000 colonies could be separated and imaged on a single Agar plate. Regions of interest were determined automatically and colonies were assigned an ID number. To avoid crowding the image only a few numbered colonies with good performers are shown. Colonies were imaged for basal starting ratio and subsequently after calcium permeabilization, for calcium induced FRET changes. The best variants are highlighted with colored rings and numbers for easy identification. Colonies marked with blue rings show the highest FRET change, green rings indicates mutants with a low starting ratio (YFP/CFP) and red rings constitute a combination between high FRET change and a favorable low starting ratio. Based on these criteria the top 1% fraction of each plate was picked. **(b)** Colony scatter plot of FRET ratio change ($\Delta R/R$) and starting ratio (YFP/CFP) of each colony on the plate. Starting ratios of about 1 and high $\Delta R/R$ were considered preferable. In this example the colonies with highest $\Delta R/R$ lie within a starting ratio of 1.5-2.5.

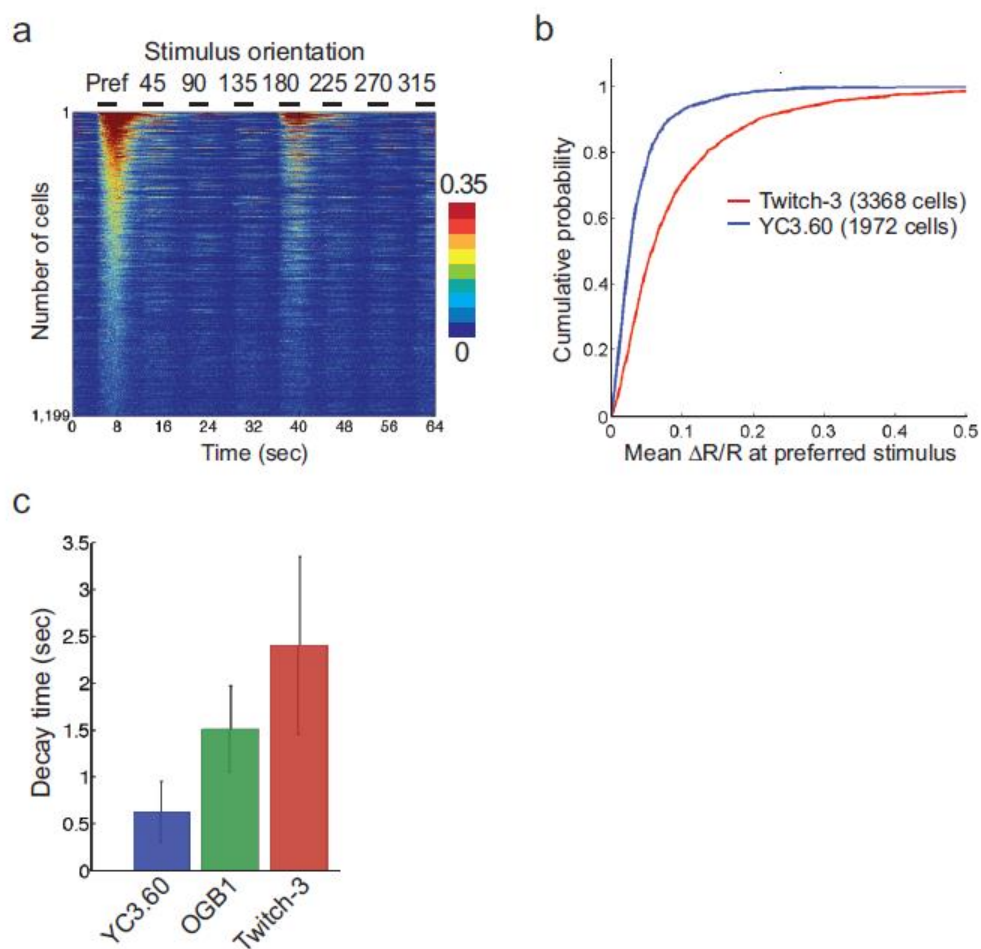
Supplementary Figure 10. Comparison of selected FRET calcium sensors in dissociated neurons



Sensor	# wells	# regions of interest	1 AP±SEM	3 AP±SEM	10 AP±SEM	160 AP±SEM
Twitch-3	14	168	5.7±0.7	12.3±1.2	33.4±2.8	194.1±15.2
TN-XXL	26	230	2.5±0.7	6.2±1.5	16.2±3.0	64.4±10.3
YC3.60	23	299	1.3±0.5	3.2±0.9	8.9±1.7	55.6±7.6
YCNano 15	16	253	5.5±1.8	11.4±2.2	23.1±3.5	83.1±6.8

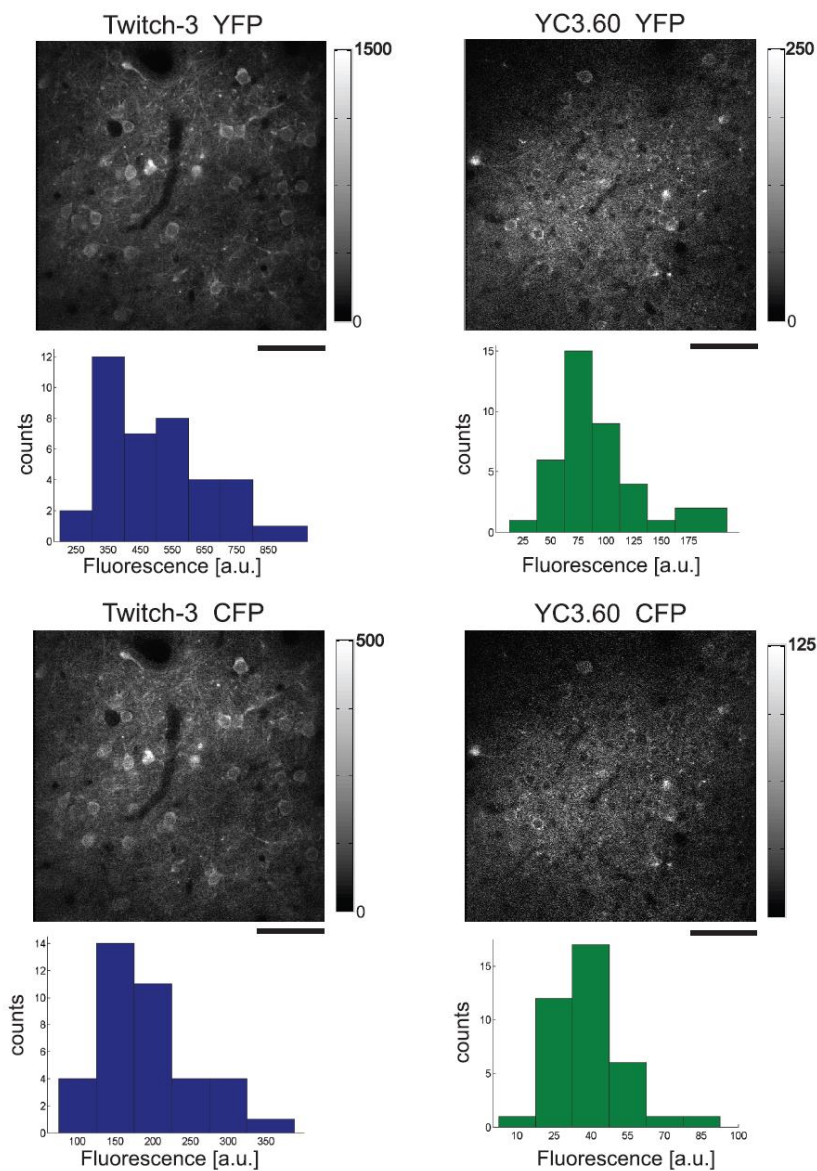
Two Troponin-C-based FRET sensors (TN-XXL, Twitch-3) and two calmodulin-M13-based FRET sensors (YC3.6, YCnano15) were compared under identical conditions. Rat primary hippocampal neuronal cultures in 96-well format were transfected by electroporation (Lonza Primary Cell Nucleofector P3 kit) of DNA constructs (3.2 micrograms). After 16 days in vitro, neurons were stimulated using a custom pair of electrodes, and responses were imaged with an Andor EMCCD camera (iXon 897, 35 fps) as previously described (Wardill et al., 2013, see Online References). Please note, however, that experimental conditions for this figure were not identical to what is described in Online Methods for Fig. 3. Different vector backbones and a different amount of DNA were used for transfection. In addition, one pair of electrodes (custom made, different than the electrodes used in Fig. 3) was used to sequentially stimulate cells in different wells.

Supplementary Figure 11. *In vivo* functional imaging of mouse visual cortex using Twitch-3.



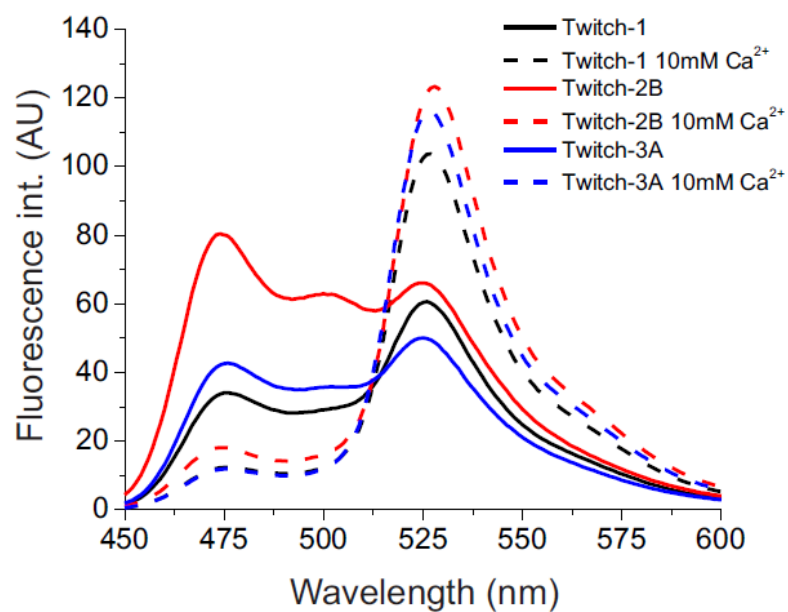
(a) Visual responses ($\Delta R/R_0$) of 1199 responsive cells, rank ordered by signal level, to eight orientations aligned in columns starting with the preferred orientation for each cell. Black bars demonstrate when stimuli were presented. **(b)** Cumulative probability distribution of averaged responses to preferred orientation stimulus for Twitch-3 (3368 cells from 6 animals) and YC 3.60 (1972 cells from 5 animals). **(c)** Calculation of half decay time constants for OGB-1, YC 3.60, and Twitch-3. Left panel shows mean and standard deviation of half decay time for the 10% most responsive cells at their preferred orientation.

Supplementary Figure 12. Differences in baseline fluorescence between Twitch-3 and YC3.60 in vivo



All images were taken 150 μm under the cortical V1 surface with an average laser power of 10 mW, without any visual stimulus. Histograms show the distribution of the averaged fluorescence signal from cell bodies ($n=38$). Scale bar, 50 μm . As Twitch-3 was brighter than YC 3.60, average laser power for imaging Twitch-3 could be reduced compared to YC3.6 (20 mW and 45 mW respectively for imaging 150 μm under the brain dura) while maintaining equal brightness.

Supplementary Figure 13. Emission spectra of purified “Twitch” variants *in vitro*



Emission spectra of equimolar amounts of purified recombinant Twitch-1 (black), Twitch-2B (blue) and Twitch-3 (red) both at basal conditions (solid lines) and at calcium saturation (dashed lines). Note that the donor brightness is approximately 2 fold higher at resting state in Twitch-2B than in other variants.

Supplementary Table S1. NMR structural statistics.

NMR constraints

Completeness of resonance assignments	
Backbone (%)	99.4
Carbon β (%)	100
Residual dipolar couplings (^1H - ^{15}N)	62

Structure precision

RMSD from mean structure (residues 2-65) (Å)	
All backbone atoms	0.90
All heavy atoms	1.31

Structure quality

MOLPROBITY

Clash score	8.79 \pm 1.87
Poor rotamers (%)	0.32 \pm 0.65
MolProbity score	1.50 \pm 0.13
Residues with bad bonds (%)	0 \pm 0
Residues with bad angles (%)	0 \pm 0
C β deviations > 0.25 Å	0 \pm 0

PROCHECK

G-factors phi-psi/all dihedral angles	0.42 /0.55
Ramachandran plot statistics (%)	
Most favored regions	93.4
Additional allowed regions	6.6
Generously allowed regions	0
Disallowed regions	0

Supplementary Table S2. SAXS data evaluation.

Construct	Ca ²⁺	Concentration mg/ml	Rg (nm)	Dmax (nm)	cpCitrine/CFP ₀	ΔR/R (%)
Twitch-1	+	1.6	3.14	10.56	9.74	400
	-	1.7	3.66	12.8	1.95	
TNXXL	+	0.86	3.33	11.16	3.48	260
	-	0.86	3.85	14.13	0.97	
tsL13	+	1.1	3.62	12.31	2.00	110
	-	1.1	3.66	14.5	0.97	
Twitch-0	+	1.1	3.37	10.86	10.48	130
	-	1.14	3.84	14.16	4.50	
2,1 Pro	+	1.52	3.06	9.71	6.66	230
	-	1.6	3.19	12.24	2.01	
2,2 Pro	+	1.7	3.23	10.38	4.91	290
	-	1.5	3.86	14.4	1.25	

Small angle X-ray scattering data were collected at zero calcium and at calcium saturation for several early Twitch constructs and Twitch-1, Ts-L13 (which harbors the full wild type TnC from *Opsanus tau* truncated at leucine 13), and TN-XXL. The construct 2,1 Pro is a FRET sensor that uses the minimal domain with a two prolines N-terminal linker and a 1 proline C-terminal linker amino acid, while 2,2 Pro uses two prolines on each side as linker amino acids. Rg values have been determined from analysis of the slope of the linear region ($s \cdot R_g < 1.3$) of the guinier plot $\ln(I)$ vs s^2 using PRIMUS and maximum particle diameter was determined using GNOM as described (see Putnam, C.D., Hammel, M., Hura, G.L., & Tainer, J.A. X-ray solution scattering (SAXS) combined with crystallography and computation: defining accurate macromolecular structures, conformations and assemblies in solution. *Quarterly Reviews of Biophysics* **40**, 191-285 (2007)). cpCitrine/CFP₀ describes the basal acceptor/donor emission ratio at zero calcium. ΔR/R describes the maximal FRET ratio change of each construct from zero calcium to calcium saturation.

Supplementary Table S3. Properties of selected Twitch sensors.

High affinity sensors				Cuvette					Hippocampal neurons		
Name	FRET pair	Mutations**	Linkers	YFP/CFP (R ₀)	ΔR/R (%)	Kd (nM)	Decay time (s)	Hill slope "Coefficient"	Maximum ΔR/R @ 160FPs	YFP/CFP (R ₀)	Decay time 10AP (s)
tsL13	ECFP cpCit174	TsTnC truncated at leucine 13	-	1.00	250	1300	0.15	1.22	-	-	-
Twitch-1	ECFP cpCit174	M65V	P, P	1.95	400	250	0.80	1.18	80	2.08	1.50
Twitch-2	ECFP cpCit174	K14F, M65V	DA, PIY	1.20	1000	150	2.80	1.34	209	1.21	1.81
Twitch-2B	mCerulean3 cpVenus ^{CD}	K14F, M65V	VADA, PIYP	0.80	800	200	2.80	1.31	104	1.53	2.11
Twitch-2C	mTurquoise2 cpCit174	K14F, M65V	VADA, PIYP	0.80	700	450	2.60	1.31	-	-	-
Twitch-3	ECFP cpCit174	V41P	DA, PLA	1.30	700	250	1.50	1.42	321	1.30	2.05
Twitch-3B	ECFP cpVenus ^{CD}	V41P	DA, PLA	1.15	900	150	2.98	1.13	185	1.53	2.55

Low affinity sensors (Single EF-hand)											
Name	FRET pair	Mutations**	Linkers	YFP/CFP (R ₀)	ΔR/R (%)	Kd (μM)	Decay time (s)	Hill slope "Coefficient"	Maximum ΔR/R @ 160FPs	YFP/CFP (R ₀)	Decay time 10AP (s)
Twitch-4	ECFP cpCit174	M65V , 54D+*	DA, PIY	1.20	600	2.80	0.50	1.04	100	1.40	0.615
2N1 390 54S+	ECFP cpCit174	M65V , 54S+*	DA, PIY	1.22	500	2.60	0.45	-	90	1.50	0.814
Twitch-5	ECFP cpCit174	18D+*, M65V	DA, PIY	1.25	550	9.25	0.16	1.37	-	-	-
2N1 390 18D+ B	mCerulean3 cpVenus ^{CD}	18D+*, M65V	DA, PIY	0.74	320	51.5	0.12	1.06	-	-	-
2N1 390 54S+ B	mCerulean3 cpVenus ^{CD}	54S+*, M65V	DA, PIY	0.74	330	257.0	0.07	-	-	-	-
Twitch-2B 18D+	mCerulean3 cpVenus ^{CD}	K14F, M65V, 54S+*	DA, PIY	0.80	220	139.0	0.15	-	-	-	-
Twitch-2B 54S+	mCerulean3 cpVenus ^{CD}	K14F, M65V, 54S+*	DA, PIY	0.78	320	174.0	0.07	-	-	-	-

* Amino acid insertion after the indicated numbered position, ** All sensors include the mutations N15D, D17N, N51D and D53N within the minimal domain to reduce Mg²⁺-binding.